Lab 3: Photometry With The Leuschner Infrared Camera

Andy Friedman [1,2]
December 19, 2001

ABSTRACT

In this report, we discuss the use of the Leuschner 30-inch telescope and Infrared camera to perform aperture photometry on selected stars. We measured the relevant properties of the 256×256 pixel IR camera, including saturation = 21,000 ± 1000 counts, gain = 0.050 ± 0.001 (photoelectrons/count), bias = 16 ± 2 counts, and readnoise ≈ 2 counts. We took dark images and constructed a flat field, removed the instrumental effects and then performed aperture photometry on 5 standard stars and 2 stars of unknown magnitude. Using four standard stars, we measured the conversion factor between photoelectrons per second and star brightness. With this information, we measured the apparent brightness of star HD2892, arriving at $m = 6.0 \pm 0.7$ magnitudes. Our final results are summarized in a plot that shows the theoretical and measured signal to noise ratio (SNR) per pixel at different exposure times, for stars of varying magnitude.

1. Introduction: Photometry

Photometry is the precise measurement of the brightness of stars. To measure brightness, we want to know how many photons are hitting our detector, per unit time per unit area, and convert this number to magnitudes. However, this number is often very difficult to measure directly. What we can measure, is the number of photons N that are detected in a given exposure time t in a given frequency band determined by your filter. By measuring this number again for a star of known magnitude under identical observational conditions, we can apply the technique of differential photometry to determine the brightness of our star. In order to do this, we had to become familiar with the operation of the Leuschner 30-inch robotic telescope and learn how to use the standard astronomical coordinate systems. We applied our previous knowledge of removing the instrumental affects of a pixel array detector,[3] to remove dark current, bias, and flat field the image. We learned the new technique of aperture photometry where we measure the sky background in an annulus around our star, and extract the star signal by subtracting the sky background from a small circular aperture containing the star.

---

[1] e-mail: friedman@ugastro.berkeley.edu

[2] Lab Group: Lee, Jim, Christina, and Lindsey

[3] Although the two are quite similar, the IR camera is not a CCD camera. It has a 256×256 pixel array detector rather than 512×512, and the pixel counts are read out differently.

2. Using The Leushcner 30-inch Robotic Telescope

The Leushcner 30-inch Robotic Telescope has a camera that detects infrared photons, but before we can point the telescope at any stars or other astronomical objects of interest, we have to ask ourselves the big picture question, "Is there any factor that would prevent me from seeing the star?" The answer is that there are dozens of such factors. Most are correctable and have to do with the state of the telescope apparatus itself. Others, such as unpredictable weather conditions are simply out of our control. Assuming clear skies, during an observation night[4], while taking images, one must go through the following common sense checklist.

1. log into fast to control the telescope (see the lab handout for the tx command syntax.)
2. Open the dome slit
3. Make sure the telescope is looking out the dome slit
4. Make sure the flip mirror is in the right position
5. Select the desired filter (the plug will not let any light through)
6. Adjust the secondary mirror if the image is not in focus.
7. Check to see if the telescope is pointing properly (check a known object)
8. Choose an exposure time. Short ones detect little. Long exposures may saturate.
9. Determine whether the star is in the telescope's potential field of view.

It is this last point that requires the knowledge of the major astronomical coordinate systems, as discussed in the following section.

2.1. Astronomical Coordinate Systems

Assuming everything is working on earth with the telescope, and that we can point it anywhere we choose within its range of motion, we now must ask ourselves whether the star will agree to be in our field of view at the time during the night when we would like to observe it. Answering this question requires advanced knowledge of where the star will be and this necessitates an understanding of the standard astronomical coordinate systems. After discussing them in some detail, we will include and discuss a plot that answers this question quantitatively for us. The standard coordinate systems are the equatorial (or celestial) system and the horizon system. The equatorial system assigns a position to astronomical objects on the celestial sphere, a two dimensional spherical surface that the distant stars appear to be projected onto, much like taking a photograph from the inside of a balloon. Since the stars are so distant, to good approximation, we can treat the celestial sphere as if it resides off at infinity. We then wish to relate the stars coordinates on the celestial sphere to the position in which they appear to us from a particular place and time on

[4]Only radio astronomers have the luxury of daytime observations. Infrared astronomers have to deal with the fact that the night sky is so bright in the IR, that its practically always daytime in the infrared.

earth, and this is done using the horizon system.

In general, two coordinates are needed to uniquely specify an objects position on a sphere, so since the earth and the celestial sphere are both eminently spherical, it is to our advantage to choose some convenient set of spherical coordinates. All such systems have a latitude-like and a longitude-like coordinate, almost completely analogous to latitude and longitude lines drawn on a globe of the earth. These coordinates are called right ascension and declination (RA,DEC) in the equatorial system, and Azimuth and Altitude (or Elevation) (AZ, ALT=EL) in the horizon system. Later in this section I will discuss the mathematics behind transforming between these coordinate systems and an idl program I wrote that does it for you automatically. But before doing so, it will be useful to discuss both of these coordinate systems qualitatively.

I spend a great deal on this section, even though it may not be entirely central to the lab, largely because it interests me and because I spend the better part of a week writing a general coordinate transformation program that could convert between any of the major astronomical coordinate systems. Nevertheless, I realize the description herein may be verbose and well beyond what the report calls for. In any case, please pardon the indiscretion.

2.1.1. The Horizon System

The simplest of these coordinate systems is by far the horizon system, because the reference point is defined by none other than you, the observer. The horizon system gets its name from the idea of an observer's local horizon, the great circle that bisects the earth and is perpendicular to the line drawn straight up from the observer's position, the local zenith. The coordinates used in this system are Azimuth (AZ), and Altitude (ALT) or Elevation (EL), where AZ is our longitude-like coordinate and ALT or EL is our latitude like coordinate.[5] AZ is measured in degrees eastwardly from North (AZ=0) to East (AZ=90) to South (AZ = 180) to West (AZ = 270) and back to north again at (AZ=360). Notice that AZ can never be negative. Altitude or Elevation is measured up from the horizon to your object, and reaches a maximum ALT=EL=90 degrees at the zenith. Negative ALT angles are allowed to go down as far as -90 , but this simply tells us that for observational purposes, the object is below the horizon, and is certainly not visible via any current astronomical imaging technology, x-ray vision not withstanding. Due to the earth's rotation, for stars that are visible, many will trace our arcs as they rise and set in the sky during the night, and their AZ and ALT angles will change with time, often placing the object out of the telescope's potential field of view. This debacle will be addressed in a future plot where we use these coordinates to quantitatively determine the time window in which we will be able to view a star from our remote location at Leuschner.

[5] Altitude and Elevation Angle are different names for the same thing! Much confusion arose over this in our lab, where at first we thought that EL was actually our Zenith angle, which is the 90 degree complement of ALT, measured down from the local zenith. After resolving these linguistic differences, we were able to proceed properly.

2.1.2. The Equatorial System

Having defined a coordinate system that depends on the observer's position, one might naturally ask if we can come up with one that remains independent of our location. In the equatorial system, we find one such system. As one might expect, the equatorial system uses the earth's equator and the rotation of the earth as a natural reference frame to specify coordinates. The celestial equator is coplanar with the Earth's equator, and on the celestial sphere each star has a fixed RA and DEC. If we extend the line through the north and south poles of the earth's out to infinity where they intersects the celestial sphere, we can define the north and south celestial poles. Thus even as the earth spins on its axis and orbits the sun, we can still attach fixed labels to stars we would like to keep tabs on.

As far as the coordinates themselves, a star's DEC (which is analogous to latitude) is 0 at the celestial equator and goes up to $\pm$ 90 degrees at the north and south celestial poles, respectively. Much like the time zones on earth, a star's RA (analogous to longitude), is broken up into 24 hour circles, and thus RA ranges from 0 to 24 hours, not degrees. The zero point of RA is not obvious, so we take advantage of some fortunate solar system geometry. The earth orbits the sun in the ecliptic plane which is aligned at 23.5 degrees to the earth's equator and thus to the celestial equator as well. In a year the sun appears to orbit the earth once in the ecliptic plane as projected onto the celestial sphere. The celestial equator and the ecliptic plane can be thought of as two great circles on the celestial sphere that will necessarily intersect at two points in the earth's orbit. To arbitrarily define RA=24=0 hours, we use one of these points, the vernal equinox, which happens in the spring for the northern hemisphere (March 21). Halfway in between the vernal equinox and the autumnal equinox, (the other crossing point), we arrive at the summer solstice, where the ecliptic plane rises to a maximum DEC = 23.5 degrees. Six months later at the winter solstice, the we reach a minimum of DEC = -23.5 degrees. So luckily the solar system has been kind to us in this regard, but to be fair, pretty much any solar system could be used to define some consistent set of astronomical coordinates if the aliens there are clever enough.

2.1.3. Hour Angle And Local Sidereal Time

Astronomical time units are also used in the equatorial coordinate system. The most useful of these two times are an object's Hour Angle (HA) and the Local Sidereal Time (LST). The hour angle is simply the angular distance (measured in hours) of an object right on your meridian, where the meridian is defined as a great circle on the celestial sphere that passes through the north and south celestial poles and your local zenith, which is the point directly above you in the sky. The Local Sidereal Time (LST) is defined by the fact that due to the earth's motion about the sun, the positions of stars on the celestial sphere shift in the position that they rise at night by roughly 4 minutes a day. Thus the sidereal year is slightly smaller than an earth year, for example. Knowing the HA, we can calculate the LST from the formula:

$$LST = HA + RA \tag{1}$$

It is useful to note that since we define RA=0 at the vernal equinox, and $LST = HA + RA$, at the vernal equinox, LST=HA. In addition, your RA=LST when the star you are observing is right on the meridian. This can be seen in an upcoming plot where we observe the star at an LST that is very close to the star's RA. But before that, we need to talk a bit about these coordinate systems quantitatively.

2.2. Coordinate Transformation Mathematics

Now that we have discussed much about these coordinate systems qualitatively, one might ask how we actually physically convert from one coordinate system to another. To do so, there are two major geometrical methods. One is to draw a complex diagram with the earth and the concentric celestial sphere, label all the appropriate angles, draw some triangles and relate all the angles to one another via a mess of sines and cosines. Sparing the reader this task, if we were to do so, and wanted to convert from (HA,DEC) to (AZ,ALT), for example, we would arrive at the formulas.

$$ALT = \sin^{-1}\left(\sin(DEC)\sin(\phi) + \cos(DEC)\cos(\phi)\cos(HA)\right) \tag{2}$$

and

$$AZ = \tan^{-1}\left(\frac{-\cos(DEC)\sin(HA)}{\sin(DEC)\cos(\phi) - \sin(\phi)\cos(DEC)\cos(HA)}\right) \tag{3}$$

where: ALT = altitude (or elevation EL), AZ = Azimuth, DEC = declination, ϕ = the observer's latitude on earth, HA = local hour angle, and . Note that since $RA = LST - HA$, one could easily express this mess in terms of RA. Similarly, we could easily solve the equations to apply the inverse transformation from (AZ,ALT) back to (HA,DEC)

A more useful method as far as transforming between any general coordinate system is arrived at using rotation matrices. The idea is first to convert from spherical coordinates to a vector in Cartesian coordinates, apply the relevant rotation matrix, then convert back to spherical coordinates and extract our transformed astronomical coordinates. The process is conceptually simpler and computationally more efficient, especially using idl code. I actually wrote a program which allows you to transform between any of the four astronomical coordinate systems: (RA,DEC), (HA,DEC), (AZ,ALT). and even galactic coordinates, (l,b), even though they weren't useful for this particular lab. I will not show the relevant rotation matrices here (they can be found in the references)[6], but suffice it to say we can define rotation matrices to transform from (RA,DEC) to (HA,DEC), (HA,DEC) to (AZ,ALT), and (RA,DEC) to (l,b). Using these three rotation matrices, call them $R1$,$R2$, and $R3$, for example, through suitable multiplication of these three basis matrices and their inverses, we can always construct a general transformation matrix which can perform transform any of the 12 possible transformations between the four distinct coordinate systems.

[6]They can be found in the optical lab's old website, in a coordinate transformation primer written by Carl Heiles.

I spent a great deal of time on this program because it was useful for me to see what I could learn about idl programming, and, in addition, the idea of creating a completely general coordinate transformation program just happened to sound really cool. Thanks to an error corrected due to a helpful suggestion from Nate McCrady, I am happy to say that the program has been tested and it works. It may come in handy in future labs. For anyone interested, please view the comments and code in my program named *coordtrans3*, which can be found in my home directory under the subdirectory /lab3/public. (The image below is not related to the transformation program)

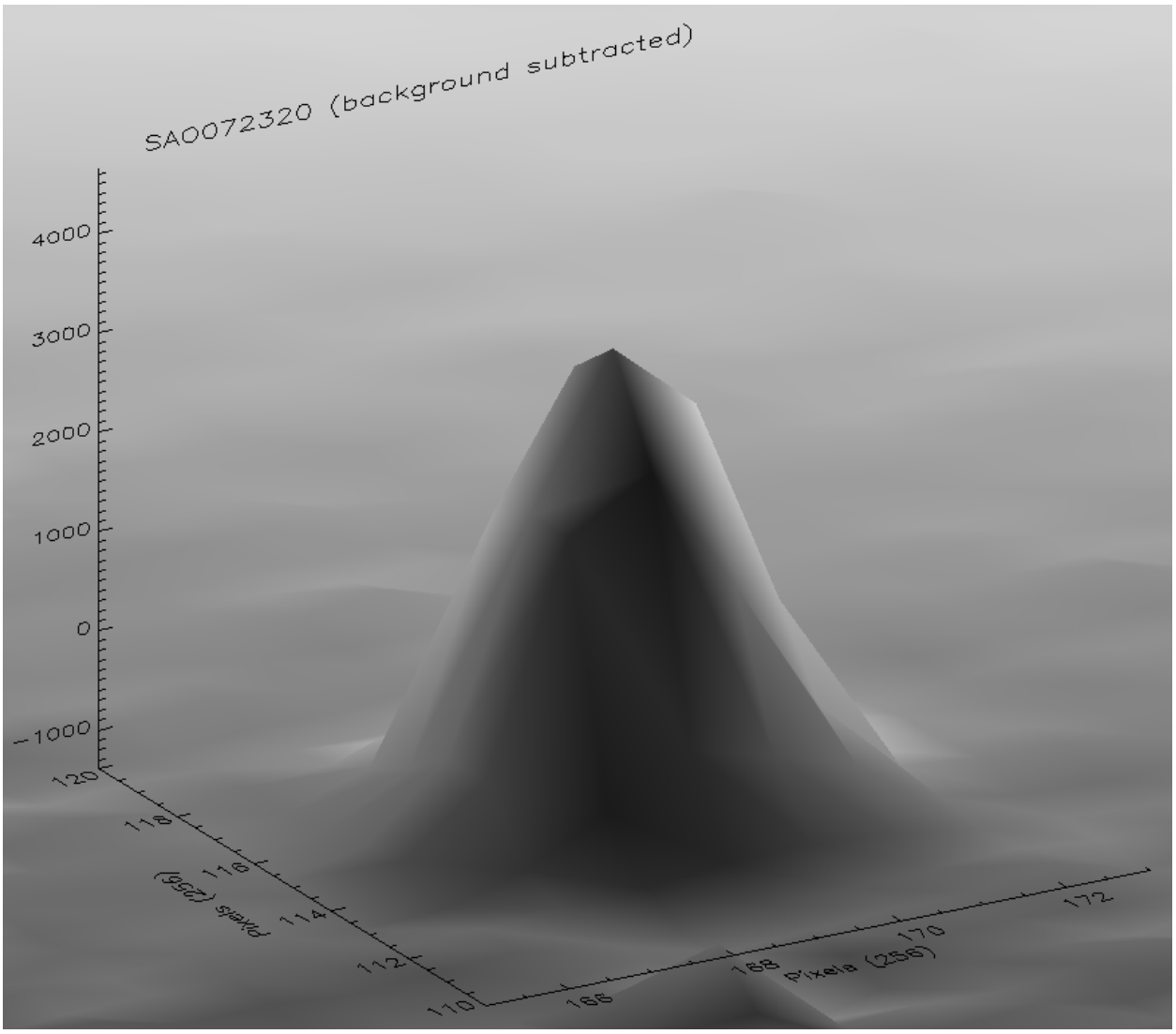

Fig. 1.— As a pure space filler for pagination convenience, check out the Gaussian profile on this star! Again, this image has nothing to do with the transformation program, this was just a good place to put it.

2.3. Plot Of Elevation Angle vs. LST

Using my transformation program, and knowing the RA and DEC for the star we wished to observe, we now can discuss a plot which quantitatively tells us whether we will be able to see that star during the time we wish to observe. Observational limits are fundamentally determined by the motion ranges of the telescope which has an HA limit of $\pm$ 2.5 hours and a DEC limit of DEC $>$ -12 degrees. So if a star has a negative Elevation angle and is below the horizon at night, our outside of our hour angle limit, then we will not be able to observe the star. A plot showing the Elevation angle as a function of Sidereal Time for our particular star illustrates these observational limits quite well, and tells us why we were indeed able to successfully observe the star.

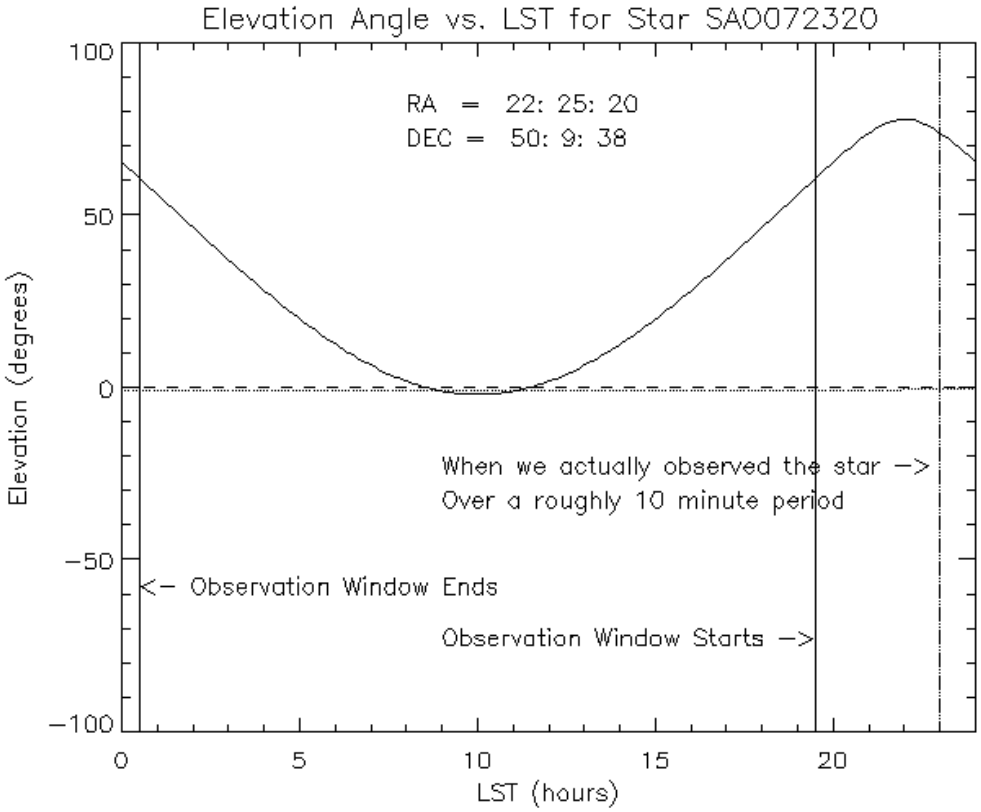

Fig. 2.— The sinusoidal curve represents the Elevation angle of our star, SAO072320, as a function of the Local Sidereal Time. Notice that the object is visible during a 5 hour time window, beginning at LST $\approx$ 20.5 hours and ending at LST $\approx$ 0.5 hours. We actually observed the star for roughly 10 minute period starting at LST $\approx$ 23 hours, which is clearly inside our search window. Notice also that the window is cyclic over a sidereal day of slightly less than 24 hours. The barely visible dotted line below the dashed line at Elevation=0 represents the star's Elevation limit as extracted from its Dec limit of DEC $>$ -12 degrees. Also Notice that the elevation angle reaches a maximum when LST = RA for our star, defining the center of our observation window. This is true in general.

3. Properties of the Infrared Camera

Much like the CCD camera we used in lab2, the IR camera is a pixel detector array that has several instrumental effects which must be removed or corrected for before one can extract a meaningful signal, which in our case, means the brightness of a star. These include the saturation, gain, readnoise, bias, Dark Current, the construction of a Flat Field, and the determination of a bad pixel mask. Most of these properties carry over from their definition in lab2, but we can discuss them here along with their relevant plots very briefly. The section discussing the construction of a Flat Field Image will be the most detailed, discussing the process mathematically, and providing an estimate of the error introduced by all the steps involved in making the Flat Field image. The bad pixel mask will be discussed later when we get to the photometry section.

3.1. Dome Saturation

The saturation is the number of counts beyond which the IR camera stops detecting any more photons. More and more photons can hit the detector but the signal will no longer increase. It occurs when the image is over-exposed. During the day, there is a sufficient amount of infrared light inside the dome to saturate the image in a few seconds, using the K-Band Filter. In the figure below, we measured this saturation by taking images of increasing exposure times, and determining at what exposure time the image saturates.

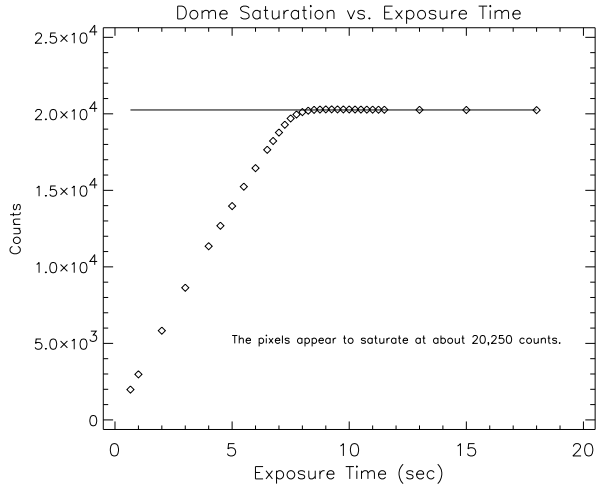

Fig. 3.— Here we close the dome during the day and plot the mean number of counts vs. exposure time for several exposure times ranging from 0 to 18s. Notice that the signal rises linearly with exposure time until a time roughly of 7s, where it develops a knee and levels out at a value of $\approx$ 20,000 counts. This saturation value is a general property of the IR camera, whereas the specific time at which saturation occurs depends on the brightness of the object. Evidently, the dome is bright enough inside during the day to saturate the image in roughly 7s.

3.2. Night Sky Saturation

If we observe the night sky, the flux of infrared light is much smaller than for the dome, and it should take much longer to reach saturation. We would expect that both a Dome Saturation image and a Night Saturation image would both saturate at the same number of pixel counts. The brightness of an object determines how fast the image saturates, but all images should saturate at the same level since it is an intrinsic feature of the IR camera. Plots of median counts vs. exposure time are plotted below for both the Dome Saturation and Night Saturation images over a wide range of exposure times.

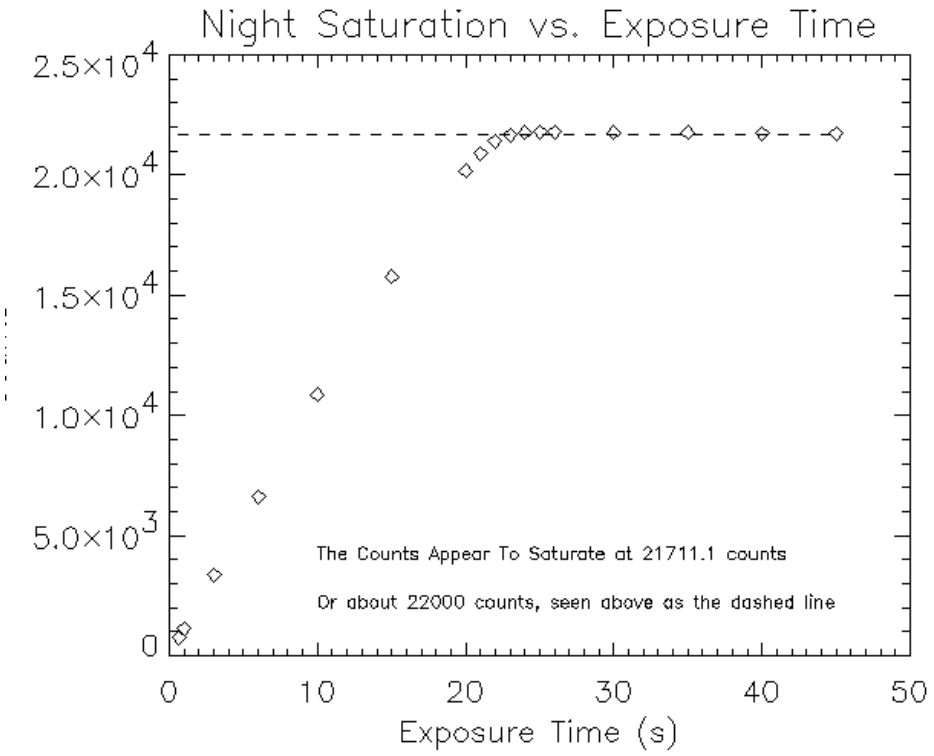

Fig. 4.— Here we took images of the night sky in star free regions at exposure times ranging from 0 to 45s, plotting the median pixel value in the array (in counts) as a function of exposure time. Unlike the Dome Saturation images, since the night sky is much dimmer, it takes much longer for the detector to saturate. We reached saturation at about 20s for the sky as compared to 7 s for the dome. Furthermore, the two saturation limits were not exactly the same, as we had expected. We got about 20,000 counts for the Dome Saturation and about 22,000 counts for the Night Saturation. We realized that it was much hotter inside the dome during the day and had measured that the temperature of the chip, $t_{chip} \approx 90K$, whereas for the night sat, t_{chip} had cooled to closer to $80K$. We hypothesized that at higher temperatures, the chip and surrounding electronics may have been compromised, enough to skew the true number of saturation counts.

3.3. Dark Current

The dark current comes from thermal noise that produces false counts at a finite detector temperature, even with the shutter closed and no image being observed. To remove these effects from our final image, we must construct a dark frame. In general, if our science exposure is 5 seconds, we need to take 5 second dark exposures. We also need to take the the dark exposures quickly after taking our raw image, so we can minimize the effects of the drifting detector temperature over time. The more darks we take, and average to make a superdark frame, the lower our error will be. If we average N dark frames, the variances add, but we reduce the noise added in constructing a single dark frame by a factor of $\frac{1}{\sqrt{N}}$. A useful question to ask is how many darks N must one take in order to increase the noise to no more that 10%. One possibility is that the noise in an individual dark frame is already less than 10% of the signal. This was actually the case for us, so we only needed N=1. When we measured the noise = $\sqrt{VOM}$ and compared it to the mean (bias subtracted) signal in just a single dark frame, we got a number on the order of $\approx$ 1%.

On the following page, we display our superdark frame and we show a 3D shade surf plot of the dark current, without bad pixels removed. The 2D and 3D images, when viewed next to one another, give you a better idea of what the dark current really looks like for the IR Camera. Pardon the waste of space. I didn't have time to figure out how to put both images side by side directly below.

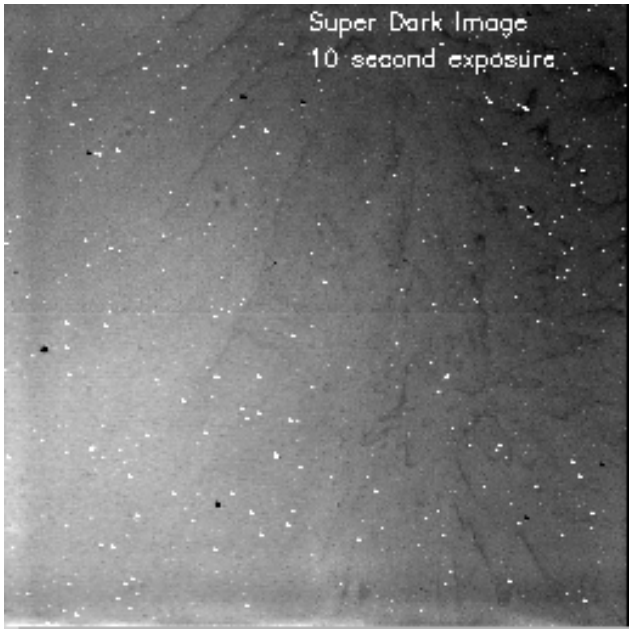

Fig. 5.— Superdark image constructed by averaging 5 darks frames, each with a t_{exp}=10s. The frothy patterns in the background are pixel to pixel gain variations that occur because this image has not yet been Flat Fielded.

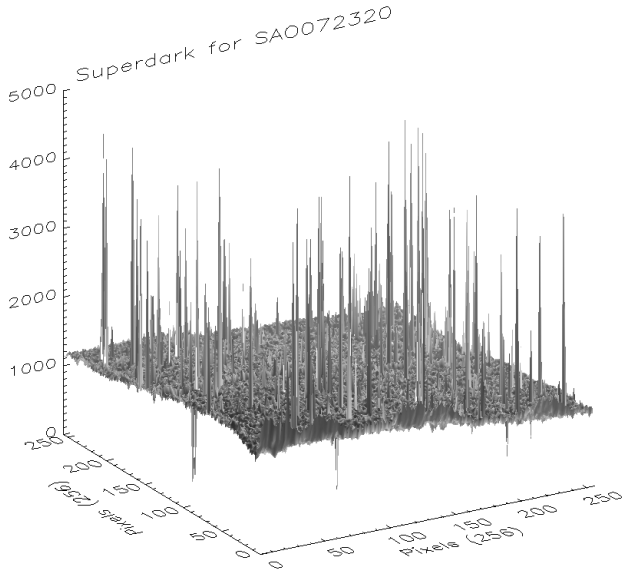

Fig. 6.— Here we show a shade surf plot of superdark. The spikes are due to bad pixels.

3.4. Bias, Gain, and Readnoise

As it was in the previous lab, the bias is the number of counts at a dark exposure time of zero, and is in place as an arbitrary offset to keep the counts in all the pixels as positive integers with values within the dynamic range of the integer data type. To measure the bias, we take dark frames of varying exposure times, do a least squares fit, and extrapolate to a counts value for and exposure time of zero. The measurements and results are summarized in the plot below.

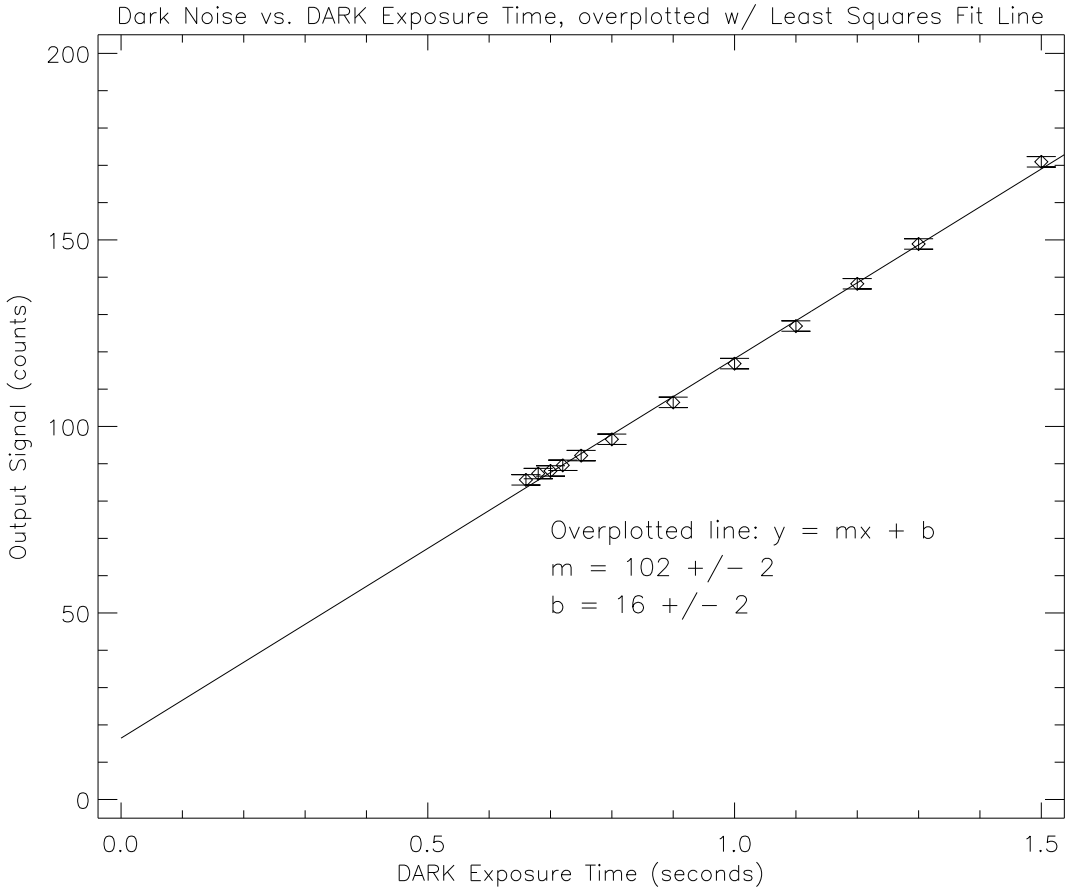

Fig. 7.— In theory, the Bias counts value occurs when the exposure time is 0. However, the minimum exposure time supported by the IR camera is 0.66s. Thus we must take several measurements at higher exposure times and extrapolate backward in time to measure the Bias. Luckily, the dark exposure counts rise linearly with exposure time, making our data very prime for a least squares fit. After performing the fit, our intercept gives us a bias value of bias = 16 counts

Again, analogous to the last lab, where we measured the gain and readnoise of the CCD using uniformly illuminated frames from the ceiling, here we use the sky as out best source of uniform illumination to measure the gain and readnoise for the IR Camera. The readnoise is an effect due to the fact that counts are measured simply in the process of trying to read off a measurement.

To measure gain and readnoise, we took 9 sky images and varied the exposure times, which we know should scale linearly with the mean number of counts. Thus we can attempt to measure the gain as in lab2 by plotting the variance vs. the mean signal counts, where we expect a positive slope straight line since the two are equal in Poisson statistics. We again use a least squares fit to measure the slope and intercept, which we determine to be the gain and the readnoise, respectively.

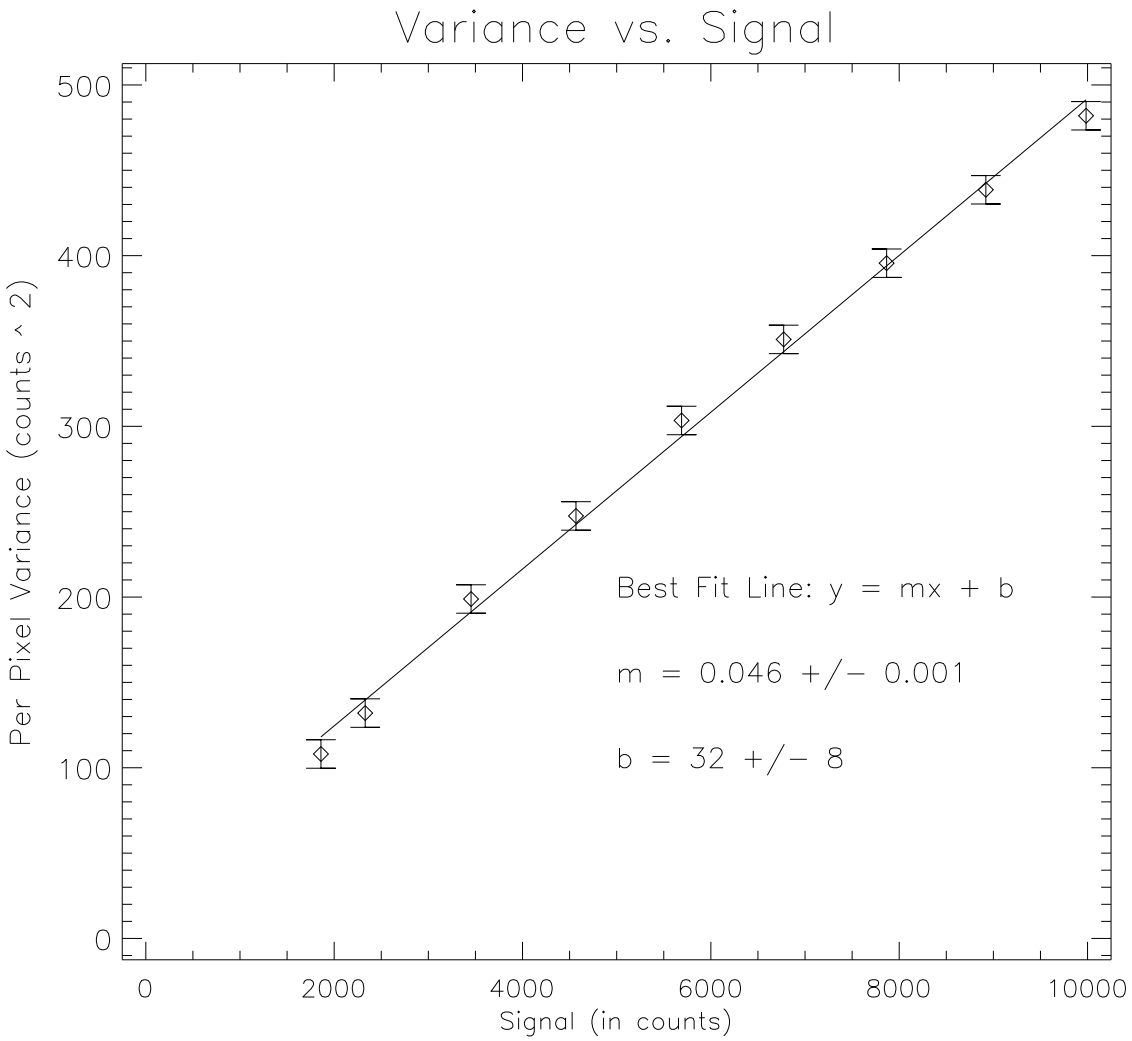

Fig. 8.— Plot of mean signal (counts) vs. variance for 9 sky images. Using our knowledge from lab2, we perform a least squares fit, that gives us our gain (slope) and readnoise (y-intercept) with errors. We arrive at final values of gain = 0.046 ± 0.001 and $\sigma^2_{RON} = 32 \pm 8$ $counts^2$. The gain (or gain factor) has units of photoelectrons/count and is a conversion factor that converts your total number of measured counts to your total number of photoelectrons. Combined with your exposure time, one can arrive at the number of photoelectrons/s hitting the detector. σ^2_{RON}, however, is measured in (counts^2) and must be multiplied by gain^2 to convert to photoelectrons^2.

3.5. FlatField

While we measured a value of gain for the IR Camera, the gain does vary by as much as $\approx$ 30% from pixel to pixel. As in lab2, in order to correct for this, we need to construct a Flat Field image that will correct for the variations in pixel gain. The Flat Field image itself is a normalized 256×256 array of varying pixel gains. We then take an image of choice and divide by the Flat Field, to correct for gain variation across the image. In lab2, we used uniformly illuminated pictures of the ceiling to construct the Flat Field. Here we will use the roughly uniformly illuminated night sky itself to construct your flat field. We actually take N=11 sky images and average them.

In general, the variation in the sky brightness B will allow us to calculate the pixel gains. If we take N images B_i, ranging from B_0 to B_{N-1}, we have N different sky brightness values. The signal in the $i-th$ frame at pixel with coordinates (x, y) will be $z_i(x, y)$. To find $z_i(x, y)$, we use this equation from the lab handout:,

$$z_i(x, y) = f(x, y)B_i + c(x, y) \tag{4}$$

Where $f(x, y)$ are the pixel gains we want for the Flat Field and the constant $c(x, y)$ is the dark current plus bias.

We now have an equation with two unknowns, B_i and $f(x, y)$. Because we are only interested in the relative gain from pixel to pixel, (i.e the Flat Field), we can subtract off the dark contribution, $c(x, y)$. To solve this system of equations approximately, we let $median(f(x, y)) = 1$, which essentially normalizes our Flat Field, and we approximate that:

$$B_i = median[z_i(x, y) - c(x, y)] \tag{5}$$

Therefore we can construct our flat field from the following:

$$FlatField = g(x, y) = \left\langle \frac{z_i(x, y) - c(x, y)}{B_i} \right\rangle \tag{6}$$

We actually calculated our Flat Field using N=11 sky images. In addition, our $c(x, y)$ was our superdark calculated using 5 individual dark frames. We wanted to make sure that these numbers were high enough so that we had taken enough data to keep the fractional error in the Flat Field below 1%. Propagating the fractional errors from Poisson noise in our sky images, dark frames, and readnoise, we arrive at the following useful formula for the fractional error in our Flat Field g:

$$\frac{\sigma_{sky}}{\langle sky \rangle} = \frac{\sqrt{{\sigma_{sky}}^2 + {\sigma_{dark}}^2 + {\sigma_{RON}}^2}}{\langle sky \rangle}$$

Where sky is the uniform sky image constructed from the average of 11 sky images. When calculated this error, we arrived at $\frac{\sigma_{sky}}{\langle sky \rangle} \approx 0.5\%$. We could have used weighted means to improve the precision of the Flat Field, but for our purposes, the fractional error was small enough that our approximate method was just fine. The figure on the following page shows the final Flat Field image.

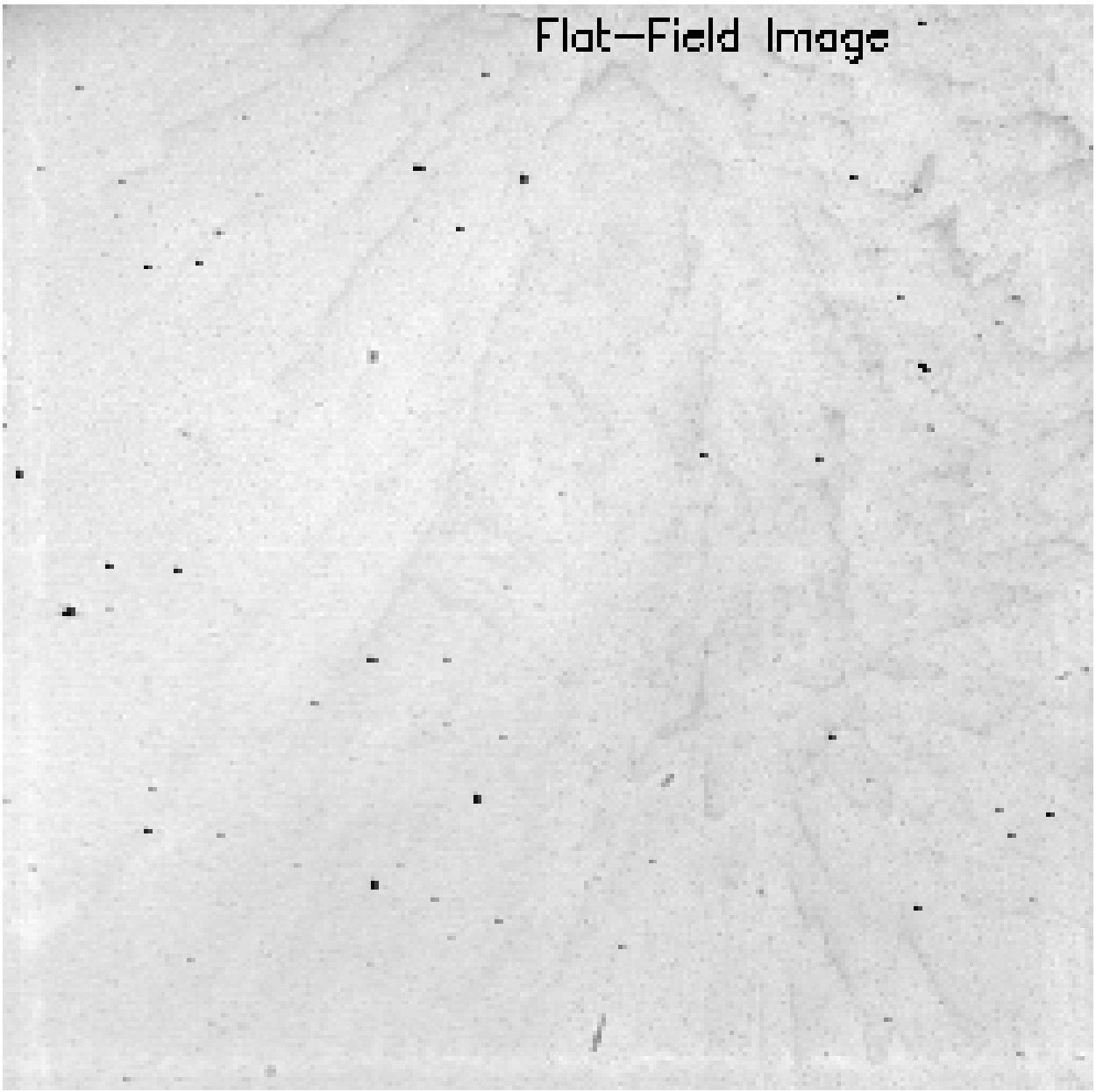

Fig. 9.— Flat Field Image Constructed using 11 sky images. Notice the mocha swirl pattern. What we are seeing is a normalized 256×256 array of varying pixel gains. If we used tvscl, and rdpix, we would find that the median value for a pixel in this image would be 1. We then take future images and we Flat Field Correct them by dividing by the Flat Field image, pixel by pixel. Notice the bad pixels that show up in black.

4. Photometry Theory: Differential Photometry

As noted earlier, Photometry is the precise measurement of the brightness of stars. To measure brightness, we want to know F_ν how many photons are hitting our detector, per unit time per unit area, and convert this number to magnitudes, where F_ν is given by. From the equation below, knowing the star's spectrum, L_ν, we can get a distance.

$$F_\nu = \frac{L_\nu}{4\pi d^2} \; watts \; m^{-2} Hz^{-1} \tag{7}$$

For a detector of Area A, frequency band $\Delta\nu$, photon detection efficiency η_ν, that measures N photons in a time t, we can also express F_ν as:

$$F_\nu = \frac{Nh\nu}{At\Delta\nu\eta_\nu} \tag{8}$$

However, this number is often very difficult to measure directly. What we can measure directly, is the number of photons N that are detected in a given exposure time t in a given frequency band determined by your filter. By measuring this number again for a star of known magnitude under identical observational conditions, we can apply the technique of differential photometry to determine the brightness of our star.

To do so, we must become familiar with the stellar magnitude system, where in general, the difference in magnitude between two stars is given by:

$$m_\nu{}^* - m_\nu = -2.5 \; log_{10}\left(\frac{F_\nu{}^*}{F_\nu}\right) \tag{9}$$

Where $m_\nu{}^*$ is the magnitude of your star, m_ν is the magnitude of your standard star, and where $F_\nu{}^*$, and F_ν represent the flux of your star and your standard star, respectively. The reference scale is defined by the star Vega, which is defined as having $m_\nu = 0$ at all wavelengths. Setting $m_\nu = 0$ in the above equation, we can write the above equation in terms of the flux of Vega, $F_{\nu 0}$

$$m_\nu{}^* = -2.5 \; log_{10}\left(\frac{F_\nu{}^*}{F_{\nu 0}}\right) \tag{10}$$

Noting that from (8), $F_\nu \propto N^*/t^*$, (where N^* is the total number of photons detected from your star and t^* is the exposure time), we can take advantage of the fact that the difference in magnitude of two stars is in terms of their flux ratio, which under identical observational conditions, allows us to cancel the terms that are difficult to measure, namely A, $\Delta\nu$, and η_ν, leaving everything in terms of N^*, t^*, N, and t, where the latter two refer to measurements made on your standard star. From these relations, and some algebra, we can see that

$$m_\nu{}^* - m_\nu = -2.5 \; log_{10}\left(\frac{N^* t}{t^* N}\right) \tag{11}$$

$$m_\nu{}^* = m_\nu - 2.5 \; log_{10}\left(\frac{N^*}{t^*}\right) + 2.5 \; log_{10}\left(\frac{N}{t}\right) \tag{12}$$

Using this equation, we can determine the magnitude of a selected star $m_\nu{}^*$, provided we also measure a standard star of known magnitude m_ν under identical conditions.

4.1. Aperture Photometry

The technique we use to measure N^* and N for both our unknown and standard stars is called aperture photometry. The key idea is that somehow, we need to count up the photons that come from the star and the star alone. Having already corrected for instrumental effects (Bias, Darks, Flat Field), we now need to correct for other sources of light which do not come from the star. In this case, that means the sky background. We already demonstrated that the night sky is quite bright in the infrared when we did our Night Saturation plot, and we now have to employ a method which will remove the sky background counts from the true star counts. Aperture photometry accomplishes this by measuring the sky background in an annulus around our star, and extracting the star signal by subtracting the sky background from a small circular aperture containing the star. It is quite simple in principle, but quite messy in practice.

4.2. Subtracting the Sky Background: Determining the Aperture and Annulus

We want to measure the total light from the star alone inside some aperture, so we need to add up all the counts in the aperture, then subtract from that aperture the median value of the sky background as measured in some annulus surrounding the aperture. This involves determining both the size of the annulus and aperture, so how do we do that? Well, first of all, what should we expect from the star alone? Since most stars have profiles that are approximately Gaussian, if the image consisted only of starlight, statistics with some messy double integrals tells us that for a 2-D Gaussian, 39% of the light will fall inside an aperture that is 1-σ in radius, 87% for 2-σ, and 99% for 3-σ. This tells us that an aperture with a radius of 3-σ will contain essentially all the light from the star. So, assuming the star has a Gaussian profile, we should always make it our goal to set the aperture radius at 3-σ.

In order to see this behavior, where we get 99% of the star light at 3-σ, we need to background subtract, so that means choosing an annulus. The idea here is to choose an annulus that surround the aperture, but the actual proper geometry to use for your annulus is not set in stone. However, there are a few major criteria. First, your annulus should not encroach upon your aperture, it should be entirely outside it. Otherwise, you will include some star light in the measurement of your sky background and that is exactly what you do not want to do. So keep the inner radius of your annulus at least at 3-σ, and probably a little bit beyond just in case we've measured σ improperly and the value we've chosen doesn't get 99% of the light at 3-σ. (We'll talk about measuring σ more in the next section.) As far as the outer radius of your annulus, in principle, you could extend it out for as long as you believe the counts inside will be a good measure of the sky background near your star. Presumably, over the 256" in your field of view, the sky background would not change tremendously, making an annulus of that size still reasonable, but eventually, if

you increase your outer radius far enough, your will reach a region where the sky background is appreciably different and the approximation will no longer be valid. Furthermore, if your outer radius happens to contain another star in your field of view, you would be measuring its starlight and skewing the value of the background, so you need to limit the outer radius to those that only contain your background.

So you have a range, with the inner radius starting just outside the aperture and the outer radius limited extended only out so far that the pixels inside the annulus get only sky background light that is a good approximation of the background level near your star. So within this range, how would one minimize the error in measuring the sky background, and thus yielding better photometry? The thing to consider here is that the more pixels you can have in your annulus within this good range, the better your measurement of the sky background will be. But for practical purposes, the worst you should do is allow the ratio of the number of pixels in your annulus to be comparable to the number in your aperture, with a ratio of about 1. Since you are subtracting the background from your aperture, you want the background measurement to be robust, and be derived from an many pixel measurements as possible. But in general, given an aperture radius R, a good rule of thumb is to set your annulus to go from, say, $2 * R$ to $3 * R$. (i.e. 6-σ to 9-σ). A figure is included below which plots the number of pixels in your annulus vs. aperture radius, for a case where the annulus always goes from R to $2 * R$. This yields an annulus/aperture pixel ratio of about 3, whereas for the $2 * R$ to $3 * R$ case, which is where we took most of our actual photometry data, we would expect a ratio of about 5.

As it turns out, the biggest difficulty we found in photometry was in actually measuring sigma, which determines our aperture radius R. First we have to find the centroid of the star, then calculate sigma based on that. Our program was fairly robust at finding the centroid, in the sense that if we defined a 30 x 30 pixel search box and made an initial guess for the centroid that was off the actual star, our program would shift the centroid back towards the its actual position. But we did notice that the value of sigma did depend on our initial guess, and that it was better if we made a better initial guess of the centroid. Of course, it was also the hardest to calculate for the fainter stars.

4.3. Photometry - Extracting the Star Signal

Now that we have an idea how to choose an aperture and annulus, how do we find the total photometric counts for our star inside our aperture? Well, we simply total all the counts from all sources inside our aperture, measure the median sky background in our annulus, take that number, multiply it by the number of of pixels in our aperture, and finally subtract that number form the original total, ultimately arriving at our total photometric counts from the star alone.

So does it work? Well, for a Gaussian profile star with Poisson noise and no sky background, the pixel sum as a function of aperture radius would asymptotically approach the star's total photometric counts, reaching 99% at an aperture radius close to 3-σ. With background noise, however, the total counts would continue to rise as the background kept contributing for larger and larger aperture radii. For this reason, in order to show that the star's true pixel sum as a function

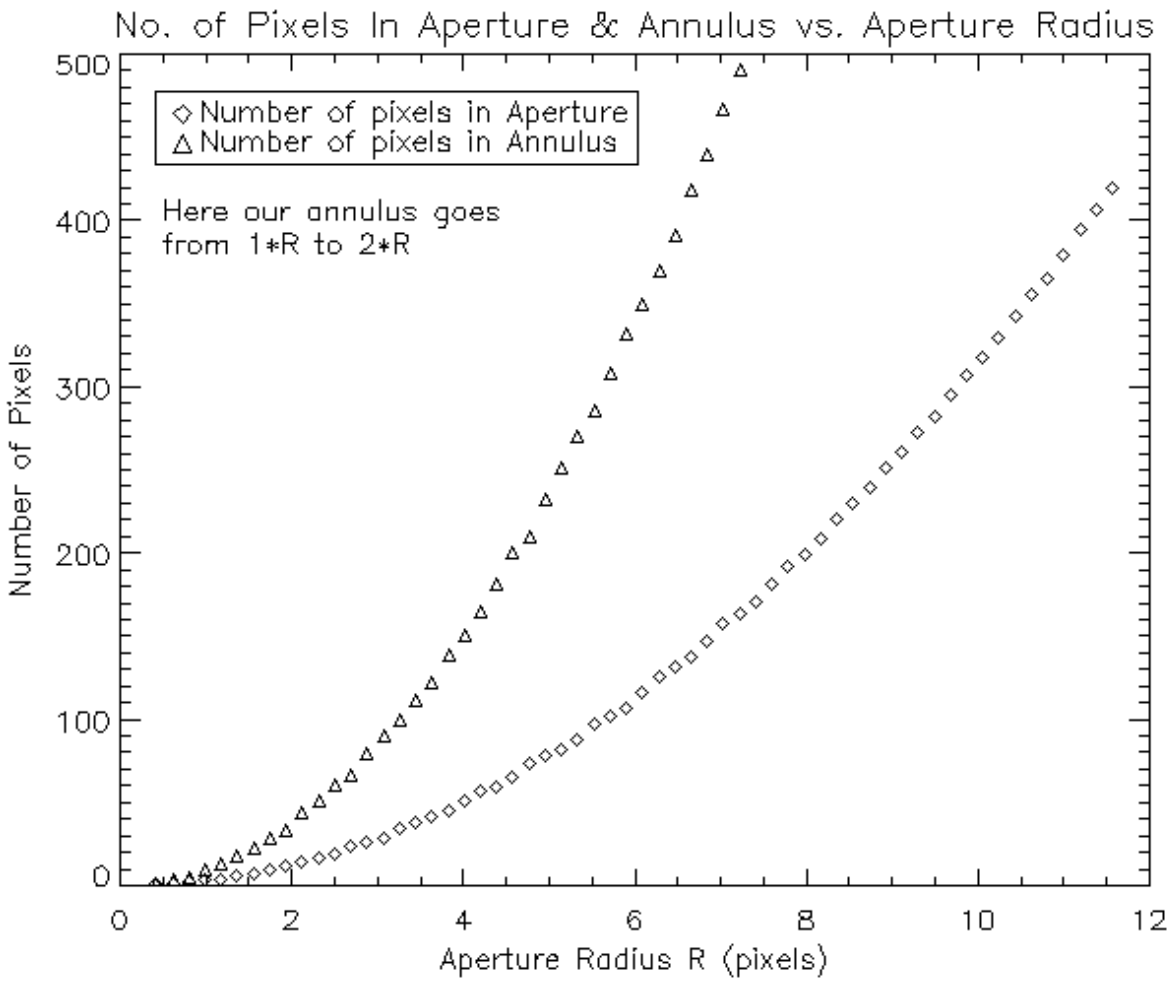

Fig. 10.— Here we plot both the number of pixels in our aperture and in our annulus as a function of aperture radius R (in pixels). (Remember that $R = 3\text{-}\sigma$.) In the above plot, we arbitrarily used an annulus that always went from R to $2R$. For accurate photometry, and a good sampling of the sky background, we require that the number of pixels in our annulus is at least on the order of the number of pixels in our aperture. For our actual photometry, we typically used annuli that went from $1.5R$ to $3R$, giving us about 5 times as may pixels in our annulus compared to our aperture. Note that the number of pixels in our aperture scales as πR^2, as expected.

of aperture radius approaches an asymptotic value, we must determine the median sky background per pixel in an annulus around the star and subtract that value from every pixel in the aperture containing the star. This is the essence of aperture photometry.

In the figure below, we perform this experiment for one of our images of the star SAO72320. We vary the aperture radius R and vary the corresponding annulus (which we arbitrarily define

from R to $2R$), determine the median sky background per pixel, and subtract it from every pixel inside the aperture. We normalize the y-axis to our total photometric counts, as measured with our eventual photometry program, and scale the x-axis in terms of sigma. Notice that the counts do indeed approach an asymptotic value, beyond which, only the Poisson noise prevents it from looking like a truly straight line at a normalized counts value of 1.

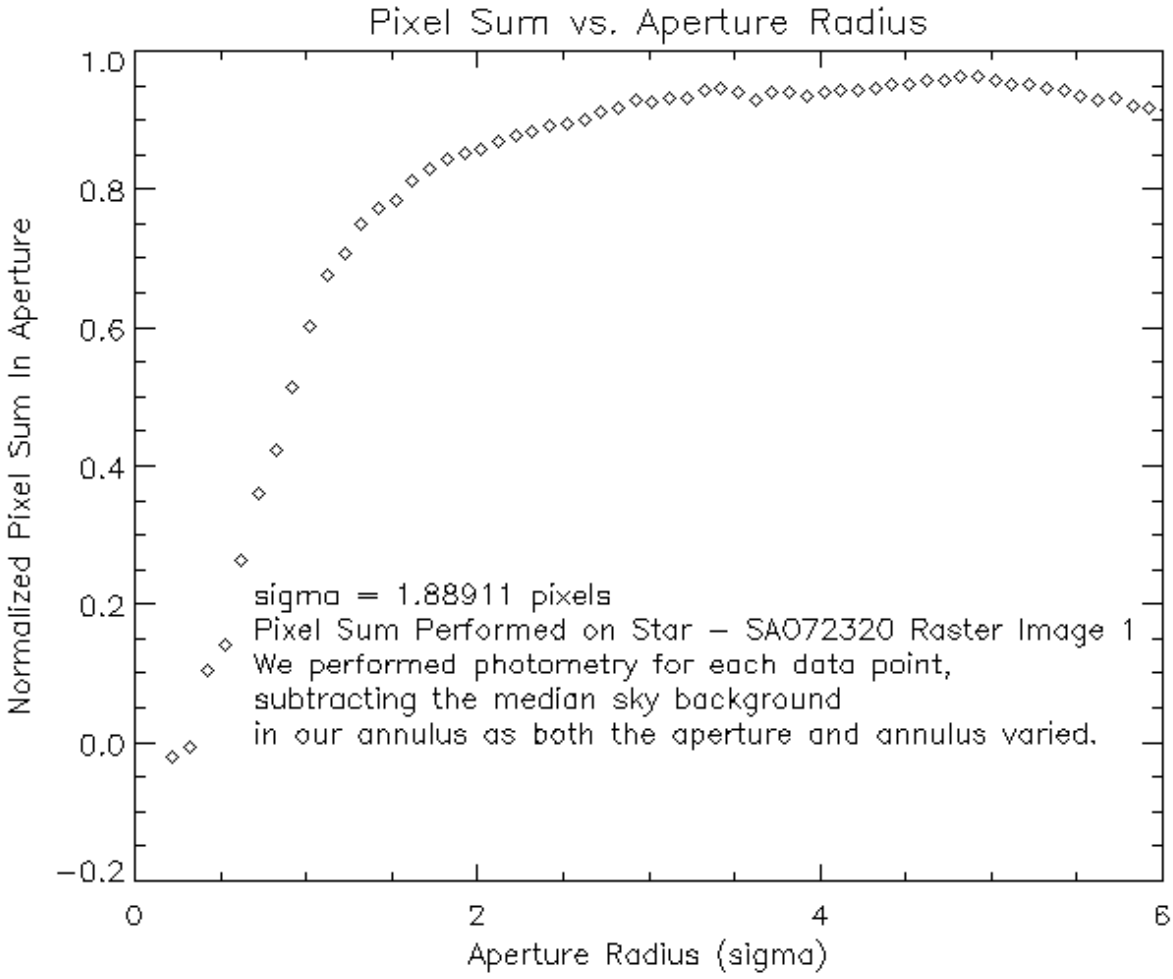

Fig. 11.— Here we plot pixel sum (normalized to the total photometric counts) vs. aperture radius for star SAO72320. We perform photometry for each data point, varying the aperture and annulus all the way out to 6-σ. The pixel sum does indeed approach an asymptotic value, showing Poisson noise at larger aperture radii. Also, at 3-σ, roughly 99% of the total starlight is included

5. Photometry Data and Analysis

We performed aperture photometry on 7 stars, 5 of known magnitude and 2 unknowns, each time taking a 9×9 raster pattern where we jogged the telescope in 40" increments. The purpose of rastering is to get more data points and to isolate the bad pixels, so we can throw out images where our star happened to land on a bad pixel. Using the 4 best standard stars, we were able to generate a plots of the conversion factor between photoelectrons/s and star brightness, and measure the magnitude of one of our unknowns, star HD 2892, arriving at $m = 6.0 \pm 0.7$ magnitudes. In the two tables directly below, we list the standard and unknown magnitude stars we used. The third table contains the data results for the photometry on all seven of these stars.

Star Designation	RA	DEC	Epoch	LST Start	LST End	K (δ_k)	Exp (s)
HD 2892	00:29:38.2	00:54:44	1950	?	?	?	1
HD 12029	01:58:41.897	29:22:47.71	2000.0	00:52:31	00:53:55	?	1

Table 1: Information for Photometric Unknown Stars Used. The K band magnitudes are unknown.

Star Designation	RA	DEC	Epoch	LST Start	LST End	K (δ_k)	Exp (s)
SAO072320	22:25:20.7	50:09:38	2000.0	23:37:47	23:45:09	8.635 (0.009)	16
FS 30 no.2	22:41:50.2	01:12:43	2000.0	00:08:17	00:13:56	10.991 (0.013)	16
SAO056596 no.0	03:38:08.3	35:10:52	2000.0	01:40:47	01:45:17	8.697 (0.012)	12
SAO056596 no.1	03:38:12.0	35:10:11	2000.0	02:06:13	02:09:27	7.570 (0.017)	8
SAO056596 no.2	03:38:08.3	35:09:38	2000.0	01:40:47	01:45:17	8.995 (0.016)	12

Table 2: Information for Photometric Standard Stars Used. K band magnitudes now given.

	SAO072320	SAO056596-2	SAO056596-1	SAO056596-0	HD2892	HD12029
Counts 1	51123.5	-30.0000	63357.2	30076.8	32775.4	168340
Counts 2	45811.2	14423.9	73724.1	33179.2	35187.5	154122
Counts 3	51676.7	23717.0	63677.8	20052.1	32442.5	160232
Counts 4	52560.2	37957.9	68364.5	33172.2	37204.2	161159
Counts 5	54174.4	11639.5	63952.2	37783.4	34699.5	162652
Counts 6	32164.2	31865.1	69931.2	22950.1	32884.6	167255
Counts 7	52544.4	32737.0	69459.4	32731.0	34965.4	127078
Counts 8	48496.9	9006.25	62640.9	31680.9	36016.0	142985
Counts 9	29713.1	16885.2	70339.4	49919.0	35718.1	154569
Mean Counts	51762.7	34186.7	64398.4	32168.0	34654.8	161189.9
SDOM	1904.96	3294.95	2270.59	1318.93	1636.50	5549.13

Table 3: Photometry Data for all stars. Individual Total Counts in Aperture for the 9 raster images, Mean Photometric counts, and SDOM values.

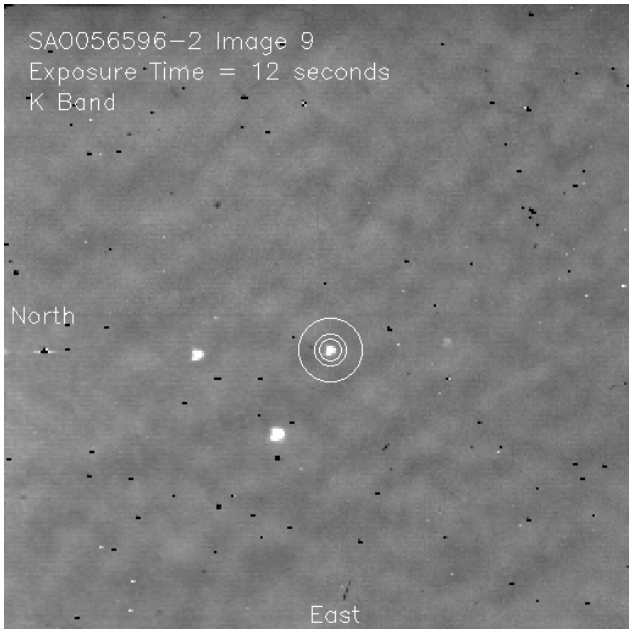

Fig. 12.— The SAO056956 star field. Overlayed around Star 2 are the photometric annulus and aperture circles used on that star for this image. Star 0 is on the upper left, and star 1, the brightest of the three is on the bottom.

We then reobserved the SAO056596 star field, shown above which contains three stars of different magnitude over a range of seven different exposure times, and performed photometry again for all three of the stars in each of the 9 raster images. We use this data to generate a plot of the measured SNR for stars of different magnitudes and exposure times. We fit this data to the theoretical curve calculated in the next section and display it as our final plot. Examples of selected images showing both the aperture and annulus used for photometry are shown in the next few pages. The actual photometric data values used to generate the SNR plots are not shown.

Star Designation	RA	DEC	Epoch	LST Start	LST End	K (δ_k)
SAO056596 no.0	03:38:08.3	35:10:52	2000.0	01:40:47	01:45:17	8.697 (0.012)
SAO056596 no.1	03:38:12.0	35:10:11	2000.0	02:06:13	02:09:27	7.570 (0.017)
SAO056596 no.2	03:38:08.3	35:09:38	2000.0	01:40:47	01:45:17	8.995 (0.016)

Table 4: We took images at varying exposure times of 2,5,7,9,11,14,and 16s for the 3 standard stars show above, each of which has a different K band magnitude. The stars happen to all be in the same field of view, which was observationally quite efficient for us. The images with higher exposure times tended to saturate (especially for the brighter of the three stars), no. 0, so we only used the first 4 exposure times as the data in our summary plots.

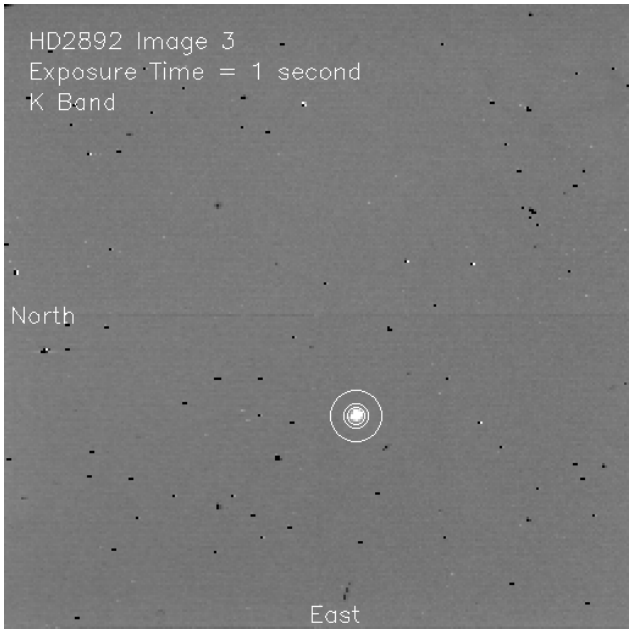

Fig. 13.— Star HD2892 Image 3 - We measure a K band magnitude for this star of $m = 6.0 \pm 0.7$

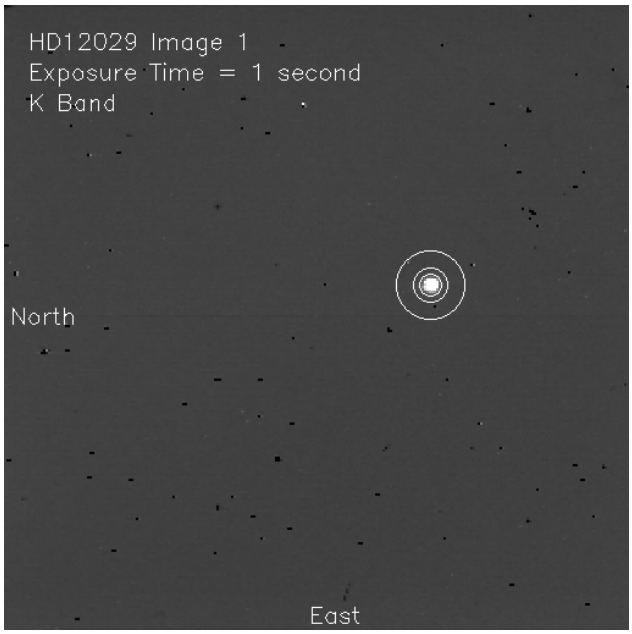

Fig. 14.— Star HD12029 Image 1 - This was our second star of unknown magnitude. Unfortunately, the initial photometric results were not good enough to allow us to measure the star's magnitude.

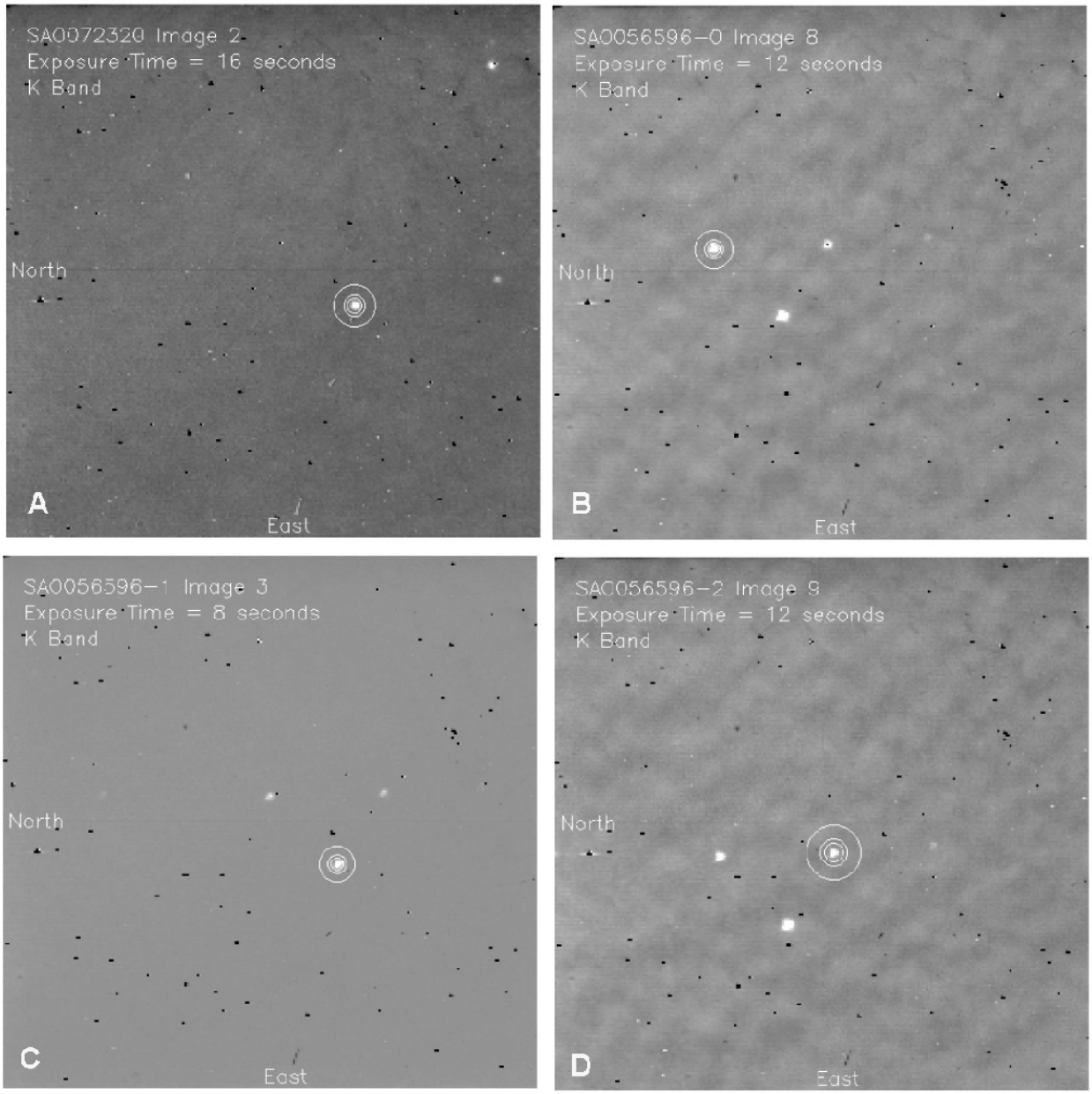

Fig. 15.— (A) SAO72320 Image 2, (B)SAO56596 star 0 Image 8, (C) SAO56596 star 1 Image 3, and (D)SAO56596 star 2 Image 9. Images are shown for photometry performed on our four good standard stars. Selected images with the relevant aperture and annuli circles are shown, with the exposure time noted on the image. Here the three SAO56596 stars in the same field of view can be compared. Photometry was performed again on all three of the SAO56596 stars for exposure times of 2,5,7,9,11,14,and 16s(not shown here) The data was used to generate our final SNR vs. texp plot for stars of different magnitudes. We performed all our observations with the K-filter, which has a Central Wavelength of 2.20 μm, a band width of 0.39 μm, and for which the flux of Vega, $F_{\nu 0} = 636 Jy$, where $1 Jy = 10^{-26}\ W\ m^{-2}\ Hz^{-1}$

5.1. Rastering

For each star we do photometry on, we jog the telescope in increments of 40", taking images in a 3 x 3 raster pattern. We do this for two major reasons. By getting 9 measurements we reduce the error in our average photometric counts for all 9 images, remembering that the SDOM = stdev/$\sqrt{N}$. Second, when you raster the image, it becomes easy to pick out the bad pixels, since they stay in the same place as the star moves. Thus when your star happens to land on a bad pixel, you can safely say that it did so and remove that data point. Furthermore, it was practically useful to do because it challenged us to understand the NSEW orientation of the images as displayed in IDL. A raster image set for star HD12029 is displayed below.

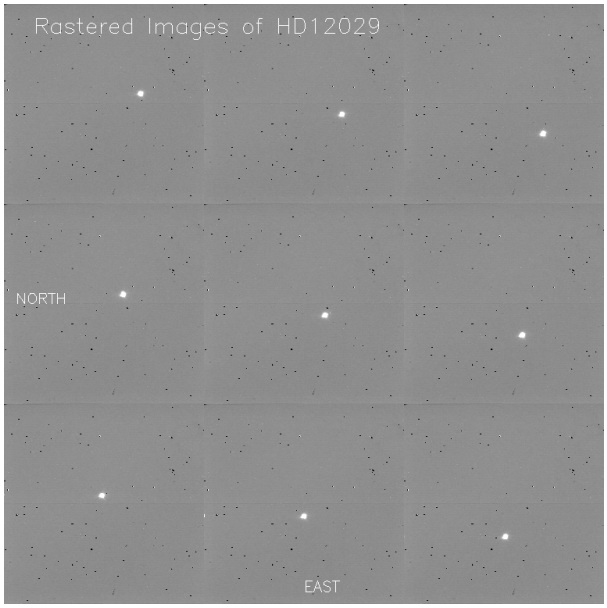

Fig. 16.— Here we display a 9 image Raster pattern of star HD12029. The center image was the first image taken. To get our 9 images we then jogged the telescope 8 times in increments of 40″ in the following pattern : N, E, S, S, W, W, N, and N. Notice that the star itself appears to move in the opposite set of directions in your field of view: S, W, N, N, E, E, S, and S. Another useful display would have been to overlay the varying star positions in the same field of view. We then would have seen the star move right, up, left, left, down, down, right, and right in our field of view.

3	2	9
4	1	8
5	6	7

Table 5: *This table summarizes the image order we used to generate the raster pattern, with the first image in the center of the 3x3 grid, the second directly above it etc...*

5.2. Bad Pixels

Bad pixels are pixels who record arbitrarily high or low numbers of counts independent of the actual number of photons hitting them per second. Such problems are often due to the electronics of how the number is read, and not always due to a "broken"pixel. Nevertheless, they must be removed to provide accurate photometry. Given a raster pattern, we can search through the 256 $\times$ 256 pixel array for pixels that are consistently at least one standard deviation away from the median value in a large number of the 9 images. We can then select these pixels and label them as bad, and create an array of good pixels that we use to perform our calculations on. An image of the bad pixel mask is shown below.

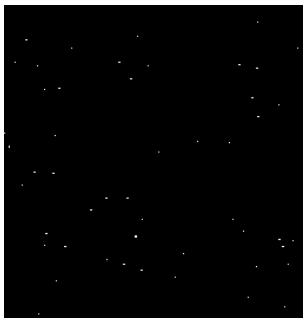

Fig. 17.— Here we display our Bad Pixel Mask for the Infrared Camera with bad pixels shown in white. Bad pixels have unstable gain properties often incorrectly arbitrarily high or low numbers of counts which could potentially throw off you photometry. After defining the bad pixel mask, we only use the good pixels in our subsequent calculations.

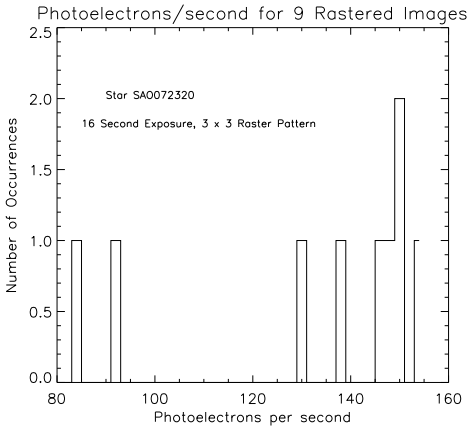

Fig. 18.— Histogram of photoelectrons per second for our 9 rastered images of star SA072320. The two images with significantly smaller photoelectrons/s likely had the star falling on a bad pixel or two. In the absence of bad pixels, the histogram would look entirely Poissonian.

5.3. SNR Theory

Having performed photometry on several standard stars of known magnitude and arrived at values their for N, the number of counts in our aperture in a given exposure time t, we need to convert N_{counts} to photoelectrons N_{pe}, to calculate the per pixel SNR. This is achieved by multiplying by the gain factor as defined earlier:

$$N_{pe} = (N_{counts})(gain) \tag{13}$$

We now would like to introduce the conversion factor K, which relates the photoelectrons per second detected by the infrared camera and the brightness (magnitude) of a star m, defined with respect to Vega. K should be a constant for all stars with magnitudes defined with respect to Vega.

$$K = \frac{N_{pe}}{t}\ 10^{0.4m} \tag{14}$$

We then use K to measure the magnitude of our unknown star, HD2892, by plotting the magnitudes of 4 of our standard stars as a function of K and m. We expect a zero slope straight line, so we apply a least squares fit to the data. We expect that K should be a constant, so we also plot the mean value of our 4 K measurements. From this plot we calculate the value of K and solve for m,having measured the number of photoelectrons/s N_{pe} for HD2892. We find that $m = 6.0 \pm 0.7$. The plot can be found below.

5.4. SNR Measured

Now, we can calculate both the theoretical value and observed value for our SNR. Eventually we will overplot our theory curve on top of our data and see how well the two match up. Through the methods of error propagation, we calculate

$$\mathrm{SNR}_{est} = \frac{(K)(t)(\ 10^{-0.4m})}{\sqrt{(K)(t)(\ 10^{-0.4m}) + (\sigma_{RON}{}^2)(gain^2)(N_{pix}) + \left(\frac{I_{dark}}{5}\right)(gain)(t)(N_{pix}) + (F_{sky})(gain)(t)(N_{pix})}} \tag{15}$$

where K is the previously mentioned conversion factor, t is the exposure time, m is the magnitude of our standard star, N_{pix} is the number of pixels contained in our aperture, $\sigma_{RON}{}^2$ is the readnoise, I_{dark} is the mean dark counts, F_{sky} is the median sky background, and gain converts from counts to photoelectrons. Normally, we would add the error from the Flat Field $\frac{\sigma_{sky}}{\langle sky \rangle}$ in quadrature along with the formula for SNR_{est}, arriving at $SNR'_{est} = \sqrt{SNR^2_{est} + \left(\frac{\sigma_{sky}}{\langle sky \rangle}\right)^2}$, but since we measured $\frac{\sigma_{sky}}{\langle sky \rangle}$ to be less that 1%, we are neglecting it in the calculation.

The observed SNR can be calculated in a considerably simpler fashion.

$$SNR_{obs} = \frac{N_{counts}}{\sqrt{\sigma_{counts}{}^2}} \tag{16}$$

where N_{counts} is the mean photon counts in the aperature and σ_{counts} is the standard deviation of the number of values of signal in the aperture. There we almost always 9 such values (for each of the nine images in our raster pattern), but there were sometimes fewer if we threw out a data point due to a bad pixel, for example.

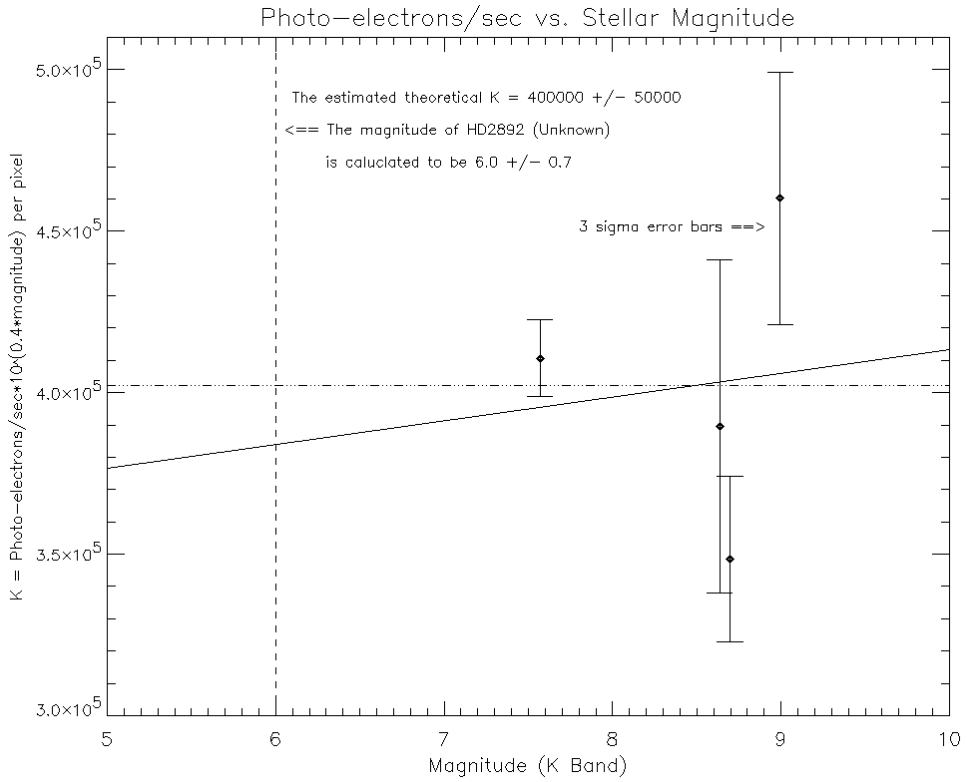

Fig. 19.— Here we plot the conversion factor K that relates the number of detected photoelectrons/s to a star's magnitude vs. magnitude, and use the fact that K should be a constant for all stars with magnitudes defined with respect to Vega, in order to measure the magnitude star HD2892. We arrive at $m = 6.0 \pm 0.7$ magnitudes. The error is arrived at via a least squares fit, and can be seen by the fact that our least squares line (dashed line) does not have zero slope, as we would expect for constant K. We only had four standard stars and four data points, so our measurements could certainly have been improved by increasing that number. We expect that with, say 100 data points, the least squares fit would approach a zero slope straight line. The error bars shown are 3-σ error bars.

We had hoped to show a plot of measured SNR vs theory curve for stars of different magnitudes and exposure times, but we were unable to finish this plot. We wrote tons of code, but it seems that there was either a hidden bug there or a problem with our data. Then we ran out of time. We considered putting in a plot that includes our false results, and explaining why they were false, but we decided against that.

Fig. 20.— SNR for stars of different magnitudes and exposure times. As the exposure time increases, so does the SNR because you have more time to collect photons from your star.

6. Conclusion

I learned a lot of practical things in this lab, that's for sure. The amazing thing is that I have been doing photometry in Alex Filippenko's group for KAIT supernovae for over a year, but I have been using mostly automatic programs and IRAF packages, which allowed me to get through the process without really understanding the fundamentals of photometry. Now I basically had to write the software from the ground up and re-invent the wheel. It makes me glad that there are already so many wheels out there. The idea of performing differential photometry because it involves measuring more tractable quantities than absolute photometry is fantastic to me, now that I finally get it. I've developed some near expert programming skills in just a few weeks as I try to survive this lab. That's probably a good thing in the long run. But I'm dying. We all are. I've been up for 46 hours straight, and not because I fell behind in any sense. That three labs and three all-nighters. That needs to stop. The problem with the lab being open all the time is that there's always something to do. So please give us more time on the next lab. Or let us do 5 rather than 6 labs for the semester. There is no way that we will not leave this lab with the skills it was designed to teach us, whether there are 5 labs or 6. We will be prepared for graduate study in astronomy or just about anything else that requires these tools. What I am talking about is not about slacking off in any sense, but striking a reasonable balance between the rest of our lives and this course. Regard us first as human beings, then as students and astronomers. Something surely can be done. I was right about one thing. Small bits of fire in the distant sky have stealthily taken over our lives.

7. Acknowledgments/References

ACKNOWLEDGMENTS

I would first like to acknowledge the support of my lab group, including Lee, Lindsey, Jim, and Christina, for pulling more all-nighters than is humanly possible. I would like to thank James Graham and Nate NcCrady for several helpful talks, and especially to Nate for pointing out an insidious stupid bug in my coordinate transformation program.

We are now all officially dead. Only a slim hope remains to revive us with sleep and pizza. The exponential growth of the work in this lab has consumed all of our lives, and it is hard to determine whether that's a good or bad thing. We shared a tremendous amount in this lab, our data, our plots, and our insights, but the work was most certainly done by all. I personally focused on the general coordinate transformation program, the actual program that does all of the photometry from the ground up, and the pixel sum vs. aperture radius program. I also wrote a lot of other code that I'm too tired to mention. I would like to thank Lee especially for sharing the programming load, and Jim, Lindsey, and Christina for doing most of theconstructing our Flat Fields, performing the gain and bias measurements, and making our darks. Lee's star raster program was also very helpful when we were observing. We all took turns operating the telescope. We seriously probably wrote a total of 50 programs in this lab. Three that I wrote were over 400 lines, and they were compact! Jim and Lindsey were instrumental throughout for just about everything, and Christina did a lot of work near the end measuring the magnitude for our unkown star and helping to organize our files. I would like to thank Eric, John, and Shane for helpful discussions. I would like to thank my body for not collapsing, and my brain for still keeping a few neurons open for business.

REFERENCES

1. Taylor, John R., *An Introduction to Error Analysis.* University Science Books, Sausalito, CA 1997, 2nd ed.

2. Woan, G. *The Cambridge Handbook of Physics Formulas* Cambridge University Press, 2000. pg. 177

3. Graham, James R., *ERRORS & STATISTICS: Ay 122 Lab Notes*, 2001

4. Graham, James R., *Lab 3 Handout*, 2001

5. Heiles, Carl, *AY120 CHEAT-SHEET FOR SPHERICAL COORDINATE TRANSFORMATION*